

State- versus Reaction-Based Information Processing in Biochemical Networks

Anne-Lena Moor^{1,2,*}, Age Tjalma³, Manuel Reinhardt³, Pieter Rein ten Wolde^{3,*}, and Christoph Zechner^{4,1,2,*}

¹Max Planck Institute of Molecular Cell Biology and Genetics, 01307 Dresden, Germany

²Center for Systems Biology Dresden, 01307 Dresden, Germany

³AMOLF, Science Park 104, 1098 XG Amsterdam, Netherlands and

⁴Scuola Internazionale Superiore di Studi Avanzati, 34136 Trieste, Italy

(*moor@mpi-cbg.de)

(*tenwolde@amolf.nl)

(*czechner@sissa.it)

Trajectory mutual information is frequently used to quantify information transfer in biochemical systems. Tractable solutions of the trajectory mutual information can be obtained via the widely used Linear-Noise Approximation (LNA) using Gaussian channel theory. This approach is expected to be accurate for sufficiently large systems. However, recent observations show that there are cases, where the mutual information obtained this way differs qualitatively from results derived using an exact Markov jump process formalism, and that the differences persist even for large systems. In this letter, we show that these differences can be explained by introducing the notion of reaction- versus state-based descriptions of trajectories. In chemical systems, the information is encoded in the sequence of reaction events, and the reaction-based trajectories of Markov jump processes capture this information. In contrast, the commonly used form of the LNA uses a state (concentration) based description of trajectories, which contains, in general, less information than a reaction-based description. Here, we show that an alternative formulation of the LNA that retains the reaction-specific information of trajectories can accurately describe the trajectory mutual information for large systems. We illustrate the consequences of different trajectory descriptions for two common cellular reaction motifs and discuss the connection with Berg-Purcell and Maximum-Likelihood sensing.

Introduction. Accurately responding to time-varying signals is essential for many natural and engineered systems, ranging from neural and biochemical networks to electronic circuits. The central measure for quantifying information transmission via time-varying signals is the information transmission rate, also called trajectory- or path mutual information rate [1–4]. Mathematically, it is defined as the rate at which the path mutual information between the input and output signal trajectories increases with the duration of these trajectories in the long-time limit. For systems without feedback, the path mutual information is identical to the history dependent transfer entropy [5]. In contrast to other information theoretical measures, such as the instantaneous or time-lagged mutual information [6], the path mutual information not only captures the accuracy of the instantaneous input-output mapping, but also the effect of temporal correlations within the input and output signals.

Cellular signalling networks show that the encoding of information in trajectories can be highly non-trivial. These systems transmit information via chemical reactions between discrete molecules. In the limit that these systems are well mixed, they are appropriately described as discrete Markov jump processes. Yet, it is commonly believed that continuous, Gaussian approximations become accurate when the reactions are linear and the copy numbers are large [7–9]. They can indeed accurately predict the instantaneous mutual information, even when the copy numbers are as small as 10 [7]. For this reason, a Gaussian approach like the Linear-Noise Approximation is frequently used to compute the information transmission rate [2, 10]. However, it has recently been shown that this Gaussian approach not only significantly underestimates the information rate, but can, in some situations, also lead to qualitatively different behaviour, even when the copy numbers are large and the instantaneous mutual information is

correctly predicted [11, 12]. This observation raises the question how information is encoded in trajectories and how this information can be quantified.

In this work, we introduce the notion of reaction- versus state-based descriptions of trajectories. We show that the common formulation of the Linear Noise Approximation (LNA) entails a state-based path description, where information is transferred via copy number/concentration fluctuations. Yet, in cellular systems the information on the input is encoded in the sequence of reaction events of the output. The discrete trajectories of the Markov jump processes capture this encoding by the reaction events, while the state-based LNA does not. The discrete reaction-based trajectories contain, in fact, more information than the corresponding continuous state-based trajectories, explaining why the Gaussian model significantly underestimates the rate for any copy number. This observation naturally leads to an alternative formulation of the LNA, the Reaction-based LNA (RNLA), which is a continuous description but explicitly keeps track of the individual reaction events (see Fig. 1). We show that this description accurately predicts the path mutual information rate for linear chemical systems at large copy numbers. In the large copy number limit the principal difference between the commonly employed state-based LNA and the Markov jump process is indeed not the discreteness of molecules but the encoding of information in reaction events rather than concentrations. Finally, we demonstrate that the distinction between reaction- versus state-based trajectories has ramifications for information transmission in cellular systems, by analyzing systems that can harness the information that resides in the reaction events.

Stochastic Reaction Dynamics. We consider a well-mixed reaction system of size Ω , consisting of M chemical species Z_1, \dots, Z_M . These species interact via K distinct reaction chan-

nels. The state of the system is denoted by the vector $z(t)$ which contains the copy numbers of the respective species at time t . To each reaction channel k , we associate a rate function $h_k(z(t))$ and define $h(z) = (h_1(z), \dots, h_K(z))^T$ and $H(z) = \text{diag}(h(z))$. For sufficiently large systems, we can make use of the approximation $z(t) = \Omega \hat{z}(t) + \delta z(t)$, where $\hat{z}(t)$ is the macroscopic mean concentration of $z(t)$ and $\delta z(t)$ is a random fluctuation that scales with the square root of the system size $\Omega^{1/2}$ [10]. For stationary systems, the dynamics of $\delta z(t)$ satisfies

$$d(\delta z(t)) = SJ\delta z(t)dt + SH^{1/2}dw(t), \quad (1)$$

where S is the stoichiometry matrix with dimension $M \times K$, J is the Jacobian of $h(z)$ evaluated at the macroscopic mean \hat{z} and dw denotes a K -dimensional noise vector of independent, standard Wiener processes, with each element $dw_k(t)$ reflecting an individual reaction channel (see Supplementary Material (SM) A).

Reaction- Versus State-based Path Descriptions. The main difference between a reaction- and state-based path description lies in whether trajectories are defined using a K -dimensional reaction noise vector, or an M -dimensional vector describing the effective copy number noise. In Eq. (1), the matrix $SH^{1/2}$ transforms the K -dimensional reaction noise vector dw into the M -dimensional species-level noise $d\xi = SH^{1/2}dw$, summarising the net contribution of reactions to the effective change in copy numbers. Since the linear combination of two Gaussian processes is again a Gaussian process, $d\xi$ remains a vector of standard Wiener processes with a modified covariance structure. For instance, the sum of two independent Gaussian increments $adw_1(t) + bdw_2(t)$ results in a single Gaussian increment $\sqrt{a^2 + b^2}dw(t)$. This projection leads to the commonly used state-based formulation of the LNA, for which trajectories are defined as $\tilde{z}_0 = \{d\xi(s) \mid 0 \leq s < t\}$.

Importantly, however, while the effective noise on a species contains the effect of *all* reactions that modify a species, the information on the input trajectory is, in general, contained only in a subset of reaction channels. The remaining reactions act as a source of uninformative noise which hampers information transfer. This observation leads to formulating the LNA based at the level of reaction channels, which we refer to as Reaction-based LNA (RLNA). In this formalism, each path is described by the individual reaction events, i.e. $\tilde{z}_0 = \{dw_k(s), k \in \{1, \dots, K\} \mid 0 \leq s < t\}$, and hence, contains the complete information available. This reaction-based path description distinguishes individual reaction events and is, hence, analogous to jump processes, where paths are unambiguously defined by the sequence of reaction times and types. In the following, we will show that the previously observed discrepancies between the Gaussian and discrete path mutual information can be explained by the difference in defining paths in the linear noise regime, i.e. either via the state- or the reaction-based formalism.

Path Mutual Information for Gaussian Processes. The calculation of mutual information between Gaussian trajectories has been studied extensively [13–15]. Let $x(t)$ and $y(t)$ be the copy numbers of two chemical species that are part of

the system state $z(t)$. The path mutual information between trajectories of $x(t)$ and $y(t)$ is generally defined as

$$I_t^{xy} = \left\langle \log \frac{dP^{xy}}{d(P^x \times P^y)} \right\rangle, \quad (2)$$

where the term inside the logarithm is the Radon-Nikodym density of the joint path measure P^{xy} with respect to the product of the marginal path measures $P^x \times P^y$ [16]. Using the expressions for the Radon-Nikodym density for Wiener processes [16], we can evaluate Eq. (2) for both state- and reaction-based paths. As derived in SM E, the mutual information between state-based paths $\tilde{x}_0 \subset \tilde{z}_0$ and $\tilde{y}_0 \subset \tilde{z}_0$ reads

$$\begin{aligned} I_t^{xy} = & \frac{1}{2} \int_0^t \sum_{k \in R_x} \frac{s_{x,k}^2}{\sigma_x^2} \left(\langle \text{Var}[\lambda_k(z(s)) \mid \tilde{x}_0] \right. \\ & \left. - \langle \text{Var}[\lambda_k(z(s)) \mid \tilde{x}_0, \tilde{y}_0] \rangle \right) \\ & + \sum_{k \in R_y} \frac{s_{y,k}^2}{\sigma_y^2} \left(\langle \text{Var}[\lambda_k(z(s)) \mid \tilde{y}_0] \right. \\ & \left. - \langle \text{Var}[\lambda_k(z(s)) \mid \tilde{x}_0, \tilde{y}_0] \rangle \right) ds, \end{aligned} \quad (3)$$

where $\lambda_k(z(t)) = \sum_{z_i} \partial_{z_i} h_k(z(t)) \delta z_i(t)$, $i \in \{1, \dots, M\}$, $\sigma_x = \sqrt{\sum_{k \in R_x} s_{x,k}^2 h_k(\hat{z}^*)}$ and $\sigma_y = \sqrt{\sum_{k \in R_y} s_{y,k}^2 h_k(\hat{z}^*)}$ denote the standard deviation of the copy numbers of $x(t)$ and $y(t)$, respectively, $s_{x,k}$ and $s_{y,k}$ the stoichiometric coefficients of reaction k modifying $x(t)$ and $y(t)$, respectively, and \hat{z}^* is the steady state of the macroscopic mean. The standard deviations σ_x and σ_y are determined by the sets of reactions R_x and R_y that affect $x(t)$ or $y(t)$, respectively. In contrast, the sums in

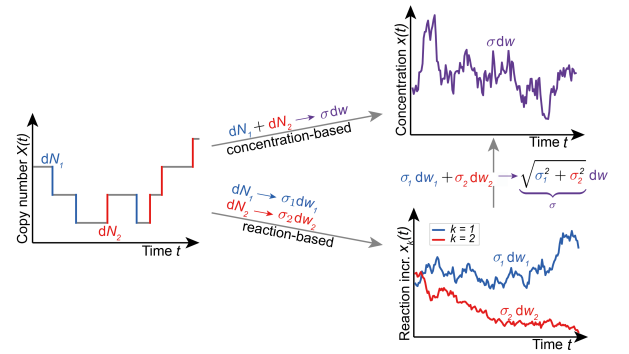


FIG. 1. State- versus reaction-based trajectories. The exemplary discrete trajectory on the left consists of two types of chemical reactions, a degradation reaction (blue) and a birth reaction (red). The reaction-based continuous formalism takes the continuous limit of each reaction counter individually, whereas the state-based formalism takes the continuous limit of the effective sum of the reaction counters. When the information is encoded in one of the two reactions, the state-based formalism underestimates the information rate.

Eq. (3) run over the subsets $R_x \subseteq R_{\bar{x}}$ and $R_y \subseteq R_{\bar{y}}$, which contain the reactions that affect $x(t)$ or $y(t)$, respectively, but are caused by species other than $x(t)$ or $y(t)$ [13–15], as discussed further below.

Evaluating Eq. (2) for reaction-based paths $x_0^t \subset z_0^t$ and $y_0^t \subset z_0^t$ instead, yields a different equation for the path mutual information (SM D):

$$I_t^{xy} = \frac{1}{2} \int_0^t \sum_{k \in R_x} \frac{\langle \text{Var}[\lambda_k(z(s)) | x_0^t] - \langle \text{Var}[\lambda_k(z(s)) | x_0^t, y_0^t] \rangle}{\sigma_k^2} + \sum_{k \in R_y} \frac{\langle \text{Var}[\lambda_k(z(s)) | y_0^t] - \langle \text{Var}[\lambda_k(z(s)) | x_0^t, y_0^t] \rangle}{\sigma_k^2} ds, \quad (4)$$

where $\sigma_k = \sqrt{h_k(\bar{z}^*)}$ denotes the standard deviation of reaction k . Note that the rate of information transmission in both cases is given by the integrands of Eq. (3) and Eq. (4).

Comparing Eq. (3) and Eq. (4) highlights important differences in the information transfer between state- and reaction-based paths. For state-based paths, the mutual information between species X and Y involves *all* reactions that change the copy numbers of these species. This is reflected in the denominators of Eq. (3), which contain effective standard deviations σ_x and σ_y with contributions from all reactions in $R_{\bar{x}}$ and $R_{\bar{y}}$. In contrast, each term in the sums of Eq. (4) is accompanied by a reaction-specific standard deviation σ_k . This is because in the reaction-based description, only subsets of reactions $R_x \subseteq R_{\bar{x}}$ and $R_y \subseteq R_{\bar{y}}$ are considered, namely those that explicitly contribute to information transfer. For example, in the reaction network $Y \rightarrow X$, $X \rightarrow \emptyset$, both reactions belong to $R_{\bar{x}}$ and indeed contribute to σ_x , but only the first reaction is also contained in R_x , since only that reaction contributes directly to information transfer from Y to X . Reactions, that are contained in $R_{\bar{x}}$ but not in R_x do contribute to information transfer, but only implicitly via their effect on the expected conditional variances. The different reaction sets are illustrated in SM C.

Calculation of the Path Mutual Information. The calculation of the path mutual information for state- and reaction-based paths requires knowledge of the expected conditional variances that show up in Eqs. (3) and (4). The conditional variances inside the expectations are the second moments of a so-called filtering distribution, which captures the statistics of a subset of the species at time t , given a complete trajectory of the remaining species between time zero and t . For the calculation of $\text{Var}[\lambda_k(z(t)) | x_0^t]$ in Eq. (4), for instance, we need the probability distribution $\pi^x(\bar{z}, t) = P(\bar{z}(t) = \bar{z} | x_0^t)$, where $\bar{z}(t)$ contains the copy numbers of all species except $x(t)$. In the case of state-based paths, the second moments of the filtering distribution are readily available through the well-known Kalman-Bucy filter, which requires the system to be in the form of a linear Gaussian state-space model [17, 18]. Taking the expectation of the resulting conditional variances gives the mutual information from Eq. (3). Note that the method presented by Tostevin and ten Wolde in [2] provides an equivalent solution to the same problem in the frequency domain.

Calculating the reaction-based path mutual information from Eq. (4) is, however, less straightforward because the

standard Kalman-Bucy filter cannot be applied [18, 19]. We therefore derived a stochastic differential equation, which describes the time-evolution of the filtering distribution in the reaction-based formalism (see SM F). For the conditional distribution $\pi^x(\bar{z}, t)$ as defined above, for instance, this equation reads

$$d\pi^x = \mathcal{A} \pi^x dt - \sum_{j \in R_{\bar{x}} \cap R_{\bar{z}}} s_{\bar{z}, j}^T \sigma_j \partial_{\bar{z}} \pi^x dw_j(t) + \sum_{k \in R_x} \frac{\lambda_k(\bar{z}, x(t)) - \langle \lambda_k(\bar{z}(t), x(t)) | x_0^t \rangle}{\sigma_k} \pi^x dw_k(t) \quad (5)$$

where \mathcal{A} is the Fokker-Planck operator prescribed by the LNA, $s_{\bar{z}, j}$ the stoichiometric change vector of reaction j acting on \bar{z} and $R_{\bar{z}}$ denotes the set of reactions that change $\bar{z}(t)$. Note that for reactions in which $\bar{z}(t)$ and $x(t)$ change simultaneously, there appears an additional contribution $s_{\bar{z}, j} \sigma_j \partial_{\bar{z}} \pi^x dw_j(t)$ as these reactions cause coupled fluctuations in both $\bar{z}(t)$ and $x(t)$.

From Eq. (5), we can derive a differential equation for the expected conditional variances as they appear in Eq. (4). For the covariances $K_{ij} = \langle \text{Cov}[\bar{z}_i(t), \bar{z}_j(t) | x_0^t] \rangle$, for instance, we obtain the matrix differential equation

$$\frac{d}{dt} K = S C R^T K dt + K R C S^T dt + S \Sigma^2 S^T - (K R \bar{\Sigma}^x C + S \Sigma^x) \cdot (C \bar{\Sigma}^x R^T K + \Sigma^x S^T). \quad (6)$$

Here, S is the net stoichiometry matrix of species \bar{Z} with dimension $M_{\bar{Z}} \times K$, $M_{\bar{Z}}$ the number of species \bar{Z} and R is the reactant stoichiometry matrix with same dimensions as S . The matrix C is a diagonal matrix with the rate constants as its diagonal elements, i.e. $C_{k,k} = c_k$, Σ is a diagonal matrix with entries $\Sigma_{k,k} = \sigma_k$ and the matrices Σ^x and $\bar{\Sigma}^x$ are variants of Σ with entries $\Sigma_{k,k}^x = \sigma_k$ and $\bar{\Sigma}_{k,k}^x = 1/\sigma_k$, respectively, if $k \in R_{\bar{x}}$ and 0 otherwise. The full derivations of Eq. (5) and (6) can be found in SM F and G. Solving Eq. (6) provides expressions for the expected conditional variances, which allows us to calculate the reaction-based path mutual information in Eq. (4).

Case study (I) – Comparison of Different Network Motifs. Next, we want to illustrate the consequences of using different path formalisms in the calculation of mutual information. To this end, we calculate the path mutual information rate analytically for two common reaction motifs [2, 20] as shown in Table I using reaction-based and state-based paths. Even though the studied motifs are quite simple, the results are markedly different. For motif a, we find that the effect of reaction 3 (i.e. with rate constant c_3) is stronger for the reaction-based formalism, where the reaction contributes twice as much to the information rate as in the state-based one. Tracking the occurrence of this factor in the calculation of the path mutual information rate shows that the inclusion of reaction 4 (i.e. with rate constant c_4) in the state-based formalism is responsible for the attenuation of reaction 3 (see SM I). While only the fluctuations caused by reaction 3 carry information about the signal (species A), in the state-based description, distinguishing reaction 3 from 4 is impossible, resulting in a loss of information about the reaction events that encode the signal. Instead, in the reaction-based scheme the fluctuations caused

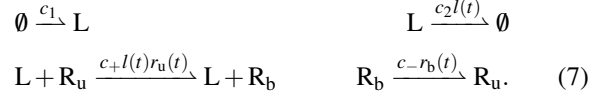
by reaction 3 can be tracked explicitly, resulting in a higher mutual information rate. In fact, summarising reaction channels into state-based paths, as done in the state-based Gaussian scheme, can only lead to a loss of information by the data-processing inequality [21]. Since reaction 4 acts purely as a (noisy) post-processing step, the mutual information rate can only decrease. Indeed, in general, reaction-based paths contain all available information, making their information rate maximal, aside from potential approximation errors arising from the LNA.

The discrepancies between the two path definitions can be much more pronounced, as can be seen from motif b. For state-based paths, the noise terms are associated with the net change in copy number of the respective species. In motif b, the reaction-specific noise terms $\sqrt{c_1}dw_1(t)$, $\sqrt{c_2a^*}dw_2(t)$, $\sqrt{c_3a^*}dw_3(t)$ and $\sqrt{c_4b^*}dw_4(t)$ are projected onto the noise terms of species A and B as $d\xi_a(t) = \sqrt{c_1 + c_2a^* + c_3a^*}dw_a(t)$ and $d\xi_b(t) = \sqrt{c_3a^* + c_4b^*}dw_b(t)$, respectively. Since reaction 3 affects both $d\xi_a(t)$ and $d\xi_b(t)$, these increments are anti-correlated at every moment in time. The path mutual information for instantly correlated copy number dynamics is ill-defined in the state-based formalism. Using the method by Tostevin *et al.*, we obtain a diverging information rate for motif b. This divergence has indeed been described previously in the analysis of transfer entropy of non-bipartite systems [22]. In contrast, in the reaction-based formalism, we keep track of the individual reactions. This leads to independent noise terms such that the information rate remains finite.

Case study (II) – Ligand-Receptor Binding. Since the reaction-based information rate is, in general, larger than the state-based rate (unless the latter is ill-defined and diverges), the question arises whether biological systems are able to access the information stored in individual reactions. To study whether this is possible, we revisit the problem of chemical sensing. In the mechanism of time integration, first analysed by Berg and Purcell (BP), the ligand concentration is estimated from the average receptor occupancy over some integration time T [23]. This receptor occupancy depends on both the ligand binding and unbinding rate. Endres and Wingreen realised, however, that only the binding events provide information on the concentration, since only the binding rate depends on the concentration [24]. This observation led to the scheme of Maximum-Likelihood (ML) sensing [24], in which the concentration is inferred from the mean duration of the unbound state of the receptor, rather than from its average occupancy. The sensing error of this ML scheme is indeed lower than that of the mechanism of time integration, by precisely a factor of 2 [23–29]. The observation that the information on the input, the ligand concentration, is encoded in one type of reaction of the receptor output, the binding reaction, suggests that the ML sensing error is related to the information rate computed for reaction-based signal trajectories. In contrast, the BP sensing error is expected to be related to the information rate of state-based paths.

To test this idea, we consider a system consisting of a time-varying ligand concentration and a receptor that senses this ligand L by switching between a ligand-bound state R_b and

an unbound state R_u as



Here, $l(t)$, $r_b(t)$, $r_u(t)$ are the copy numbers of the ligand, ligand-bound and unbound receptors, respectively. We can compute for this model the information rate in the reaction-based trajectories of the input copy number and output (ligand-bound receptor) (see SM J.1),

$$i_{rb}^r = -\frac{c_2}{2} + \frac{c_2}{2} \sqrt{\frac{2r_T c_- c_+}{c_2 c_- + c_1 c_+} + 1}, \quad (8)$$

and, similarly, for the state-based paths (see SM Eq. (J.11)). Interestingly, we can rewrite the expressions for both information rates in terms of the relative sensing error $\eta_\alpha^2 = (\delta l_\alpha / l^*)^2$, with δl_α the sensing error for ML and Burg-Purcell sensing ($\alpha = \text{ML}, \text{BP}$, respectively), and l^* the steady-state copy number. If the downstream system reads out the receptor over a time T , then the respective errors per receptor are $\eta_{\text{ML}}^2 = 1/\bar{n}_b$ and $\eta_{\text{BP}}^2 = 2/\bar{n}_b$, where $\bar{n}_b = Tp/\bar{\tau}_b$ is the average number of binding events during the time T , with $p = r_a^*/r_T$ the binding probability and $\bar{\tau}_b = 1/c_-$ the average binding time [23, 24, 29]. Since the optimal integration time T is on the order of the correlation time c_2^{-1} of the input signal [30], we take $T = c_2^{-1}$. The information rate for the two path descriptions (Eqs. (8) and (J.11)) can then be rewritten as

$$i_{rb}^r = \frac{c_2}{2} \left(\sqrt{\frac{2r_T}{\eta_{\text{ML}}^2 l^*} + 1} - 1 \right), \quad (9)$$

$$i_{sb}^r = \frac{c_2}{2} \left(\sqrt{\frac{2r_T}{\eta_{\text{BP}}^2 l^*} + 1} - 1 \right). \quad (10)$$

Interestingly, the respective expressions for the information rate differ only by the sensing error. Since the reaction-based information rate is the maximal information rate, this observation supports the idea that ML sensing can optimally extract the information that the binding reactions provide on the input concentration [24]. Noting that for this input the variance $\text{Var}[l(t)]$ is given by the mean l^* , we also see that these expressions lead to the intuitive interpretation that the information rate is determined by the speed at which independent messages are transmitted through the system, set by the correlation time c_2^{-1} of the input, times the number of messages, i.e. concentration levels, that are transmitted reliably per input correlation time, given by $\sqrt{\text{Var}[l(t)]} / (\delta l_\alpha / \sqrt{r_T})$, with $\delta l_\alpha / \sqrt{r_T}$ the absolute sensing error (see SM J.3).

Still, the question remains whether cells are able to transfer and access as much information as predicted by Eq. (9). Here, we turn to the scheme proposed by Lang *et al.* [27]. In this scheme, the cell estimates the concentration from the average receptor occupancy over some integration time T , as in the classical Berg-Purcell scheme. However, while in the classical scheme receptor unbinding is a one-step process, in the scheme of [27] the receptor, upon ligand binding, goes

Motif	Reaction	State-based rate [2]	Reaction-based rate
(a)	$A \xrightarrow{c_3} A + B, B \xrightarrow{c_4} \emptyset$	$-\frac{c_2}{2} + \frac{1}{2}\sqrt{c_2(c_2 + c_3)}$	$-\frac{c_2}{2} + \frac{1}{2}\sqrt{c_2(c_2 + 2c_3)}$
(b)	$A \xrightarrow{c_3} B \xrightarrow{c_4} \emptyset$	∞	$\frac{c_3}{2}$

TABLE I. Stationary mutual information rate between the paths of input species A and output species B of two common reaction motifs obtained via the reaction-based and state-based scheme. All motifs include the reaction $\emptyset \xrightleftharpoons[c_2]{c_1} A$. The motifs have been studied earlier in [2, 20], where motif a is referred to as motif III and motif b as motif II. The state-based information rate has been calculated using the formalism by Tostevin *et al.* [2].

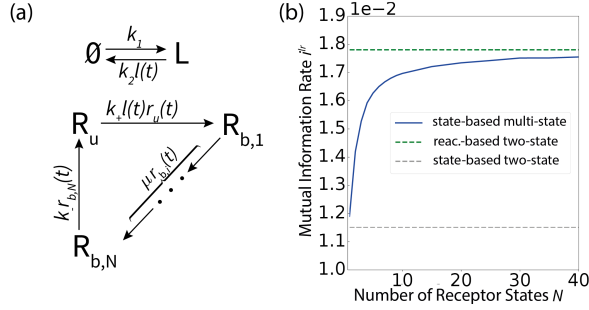


FIG. 2. Ligand-receptor binding. (a) Sketch of the multi-state receptor system. The $R_{b,i}$, $i \in \{1, \dots, N\}$ denote the ligand-bound states of the receptor. (b) Stationary mutual information rate i^r between the state-based paths \tilde{l}_0^r and \tilde{r}_0^r of the multi-state receptor dependent on the number of states N (blue solid line) in comparison to the mutual information rate of the two state receptor in the state-based description (grey dashed line) and in the reaction-based description (green dashed line). Simulations were performed with parameters $\{c_1, c_2, c_+, c_-, \mu\} = \{1, 0.01, 0.01, 50, c_-/N\}$.

through a sequence of steps before the ligand is released, such that the waiting time for ligand unbinding becomes narrower, thus reducing the contribution from the unbinding noise to the variance in the estimate of the receptor occupancy. This leads to the hypothesis that by reading out the receptor *state*, cells are nonetheless able to access the *reaction-based* information rate by eliminating the stochasticity in the unbinding of the ligand.

Calculating the state-based mutual information rate i_{ms}^r between ligand and all active states of such a multi-state receptor (SM J.4), we find that for an increasing number N of receptor states i_{ms}^r approaches i_{rb}^r in the reaction-based scheme as $N \rightarrow \infty$ (Fig. 2b). Increasing the number of receptor states,

the unbinding of the ligand becomes more predictable and the amount of accessible information increases, i.e. the state-based scheme approaches the reaction-based one. This shows that active, non-equilibrium processes can indeed make the information stored in individual chemical reactions accessible to the cell. In SM K, we present a minimal model of a linear multi-state signalling process to support the generality of this statement.

Conclusion. In summary, we introduced the notion of state-based and reaction-based trajectories and illustrated their impact on information transfer. We showed that the reaction-based information can never be smaller than the state-based one, provided that the latter is well-defined. Based on these observations, we present a formalism for calculating the mutual information between reaction-based paths using concepts from stochastic filtering. Using ideas from Maximum-Likelihood sensing, we show how the information encoded in reaction-based paths can be read out through active reaction cycles.

CODE AVAILABILITY

Python code underlying our simulations is available at https://github.com/zechnerlab/PathMI_state_vs_reaction.

ACKNOWLEDGMENTS

The authors thank Tommaso Bianucci, Avishek Das and Andreas Hilfinger for useful insights and critical feedback on this work.

-
- [1] C. E. Shannon, “A mathematical theory of communication,” *The Bell system technical journal*, vol. 27, no. 3, pp. 379–423, 1948.
 - [2] F. Tostevin and P. R. ten Wolde, “Mutual information between input and output trajectories of biochemical networks,” *Phys. Rev. Lett.*, vol. 102, p. 218101, May 2009.
 - [3] R. M. Fano, “Transmission of information: A statistical theory of communications,” *Am. J. Phys.*, vol. 29, no. 11, pp. 793–794, 1961.
 - [4] L. Duso and C. Zechner, “Path mutual information for a class of biochemical reaction networks,” in *2019 IEEE 58th Conference on Decision and Control (CDC)*, pp. 6610–6615, 2019.
 - [5] T. Schreiber, “Measuring information transfer,” *Phys. Rev. Lett.*, vol. 85, pp. 461–464, Jul 2000.
 - [6] F. Tostevin and P. R. ten Wolde, “Mutual information in time-varying biochemical systems,” *Phys. Rev. E*, vol. 81, p. 061917, Jun 2010.
 - [7] W. H. de Ronde, F. Tostevin, and P. R. ten Wolde, “Effect of feedback on the fidelity of information transmission of time-

- varying signals,” *Phys. Rev. E*, vol. 82, p. 031914, Sep 2010.
- [8] E. Ziv, I. Nemenman, and C. H. Wiggins, “Optimal signal processing in small stochastic biochemical networks,” *PLOS ONE*, vol. 2, pp. 1–16, 10 2007.
- [9] S. Tănase-Nicola and P. R. ten Wolde, “Regulatory control and the costs and benefits of biochemical noise,” *PLOS Computational Biology*, vol. 4, pp. 1–13, 08 2008.
- [10] N. G. Van Kampen, *Stochastic processes in physics and chemistry*, vol. 1. Elsevier, 1992.
- [11] A.-L. Moor and C. Zechner, “Dynamic information transfer in stochastic biochemical networks,” *Phys. Rev. Res.*, vol. 5, p. 013032, Jan 2023.
- [12] M. Reinhardt, G. c. v. Tkačik, and P. R. ten Wolde, “Path weight sampling: Exact monte carlo computation of the mutual information between stochastic trajectories,” *Phys. Rev. X*, vol. 13, p. 041017, Oct 2023.
- [13] T. T. Kadota, M. Zakai, and J. Ziv, “Mutual Information of the White Gaussian Channel With and Without Feedback,” in *IEEE Transactions on Information Theory*, vol. 17, pp. 368–371, 1971.
- [14] M. Hitsuda, “Mutual information in gaussian channels,” *Journal of Multivariate Analysis*, vol. 4, no. 1, pp. 66–73, 1974.
- [15] T. E. Duncan, “On the calculation of mutual information,” *SIAM Journal on Applied Mathematics*, vol. 19, no. 1, pp. 215–220, 1970.
- [16] R. S. Liptser and A. N. Shiriaev, *Statistics of random processes: General theory*, vol. 394. Springer, 1977.
- [17] R. E. Kálmán and R. S. Bucy, “New results in linear filtering and prediction theory,” *Journal of Basic Engineering*, vol. 83, pp. 95–108, 1961.
- [18] A. Bain and D. Crisan, *Fundamentals of stochastic filtering*, vol. 3. Springer, 2009.
- [19] A. Kutschireiter, S. C. Surace, and J.-P. Pfister, “The hitchhiker’s guide to nonlinear filtering,” *Journal of Mathematical Psychology*, vol. 94, p. 102307, 2020.
- [20] S. Tănase-Nicola, P. Warren, and P. ten Wolde, “Signal Detection, Modularity, and the Correlation between Extrinsic and Intrinsic Noise in Biochemical Networks,” *Physical Review Letters*, vol. 97, p. 068102, Aug. 2006.
- [21] T. M. Cover, *Elements of information theory*. John Wiley & Sons, 1999.
- [22] R. Chétrite, M. L. Rosinberg, T. Sagawa, and G. Tarjus, “Information thermodynamics for interacting stochastic systems without bipartite structure,” *Journal of Statistical Mechanics: Theory and Experiment*, vol. 2019, p. 114002, nov 2019.
- [23] H. Berg and E. M. Purcell, “Physics of chemoreception,” *Biophys. J.*, vol. 20, no. 2, pp. 193–219, 1977.
- [24] R. G. Endres and N. S. Wingreen, “Maximum likelihood and the single receptor,” *Phys. Rev. Lett.*, vol. 103, p. 158101, Oct 2009.
- [25] K. Kaizu, W. de Ronde, J. Pajmans, K. Takahashi, F. Tostevin, and P. R. ten Wolde, “The Berg-Purcell limit revisited,” *Biophys. J.*, vol. 106, no. 4, 2014.
- [26] W. Bialek and S. Setayeshgar, “Physical limits to biochemical signaling,” *PNAS*, vol. 102, no. 29, 2005.
- [27] A. H. Lang, C. K. Fisher, T. Mora, and P. Mehta, “Thermodynamics of statistical inference by cells,” *Phys. Rev. Lett.*, vol. 113, p. 148103, Oct 2014.
- [28] T. Mora and I. Nemenman, “Physical limit to concentration sensing in a changing environment,” *Phys. Rev. Lett.*, vol. 123, p. 198101, Nov 2019.
- [29] P. R. ten Wolde, N. B. Becker, T. E. Ouldridge, and A. Mugler, “Fundamental Limits to Cellular Sensing,” *Journal of Statistical Physics*, vol. 162, pp. 1395–1424, Jan. 2016.
- [30] G. Malaguti and P. R. ten Wolde, “Theory for the optimal detection of time-varying signals in cellular sensing systems,” *eLife*, vol. 10, p. e62574, feb 2021.